

## Research Article

# Peristaltic Flow of Non-Newtonian Fluid with Slip Effects: Analytic and Numerical Solutions

<sup>1,2</sup>M.M. Hasan, <sup>2</sup>M.A. Samad and <sup>2</sup>M.M. Hossain

<sup>1</sup>Department of Mathematics, Comilla University, Cumilla-3506, Bangladesh

<sup>2</sup>Department of Applied Mathematics, University of Dhaka, Dhaka-1000, Bangladesh

**Abstract:** This study describes two-dimensional peristaltic flow of non-Newtonian fluid through a porous asymmetric channel under the influence of the magnetic field. The slip effect is included in the model. The flow is investigated in a wave frame of reference moving with a velocity of the wave. The momentum equations are linearized using long wavelength and low Reynolds number approximation. The transformed equations have been solved numerically. Analytic solutions for stream function, velocity and pressure gradient are also obtained. The effects of various physical parameters of interest have been explained graphically. It is found that the size of the trapped bolus reduces for large value of the velocity slip parameter.

**Keywords:** Axial velocity, Casson fluid, numerical solution, peristaltic flow, slip parameter, trapped bolus

## INTRODUCTION

Peristaltic is one of the major mechanisms for fluid transport in many biological systems and industrial pumping. This property is naturally associated with a progressive wave of area expansion and contraction along the length of a fluid filled channel, mixing and transporting the fluid in the direction of the wave propagation. Peristaltic mechanism in channel has a wide range of physiological applications, for examples, urine transport from kidney to bladder, swallowing of food through esophagus, chyme movement in gastrointestinal tract, egg movement in the female fallopian tube, blood circulation in small blood vessels and water transport from ground to upper branches of tall trees. It was reported by de Vries *et al.* (1990) that the intra-uterine contraction due to the myometrial (myometrium is the middle layer of the uterine wall) contraction is peristaltic type motion and this myometrial contraction may occur in both symmetric and asymmetric directions.

Recently the study of peristaltic flow of non-Newtonian fluids through a porous medium has great attention to the researchers due to their vast applications in engineering and industry (Tripathi, 2011; Pandey and Tripathi, 2011). We know that blood in small vessels and fluids in the intestine, urine under certain conditions behave as non-Newtonian fluids. The non-Newtonian character of human blood is mainly due to the suspension of red blood cells in the plasma. But the formulation of non-Newtonian fluids is complex. So we

cannot express all non-Newtonian fluid properties in a single constitutive equation. Thus, a number of non-Newtonian fluid models have been proposed (Nadeem *et al.*, 2012). Casson fluid is one of the non-Newtonian fluids with a different character and was introduced by Casson (1959). He reported that human blood can be presented by this model. The initial work on peristaltic mechanism in a viscous fluid was conducted by Latham (1966) and after that we found many experimental studies (Nagarani, 2010; Abd-Alla *et al.*, 2013; Elangovan and Selvaraj, 2017; Mishra and Rao, 2003; Srinivas and Pushparaj, 2008; Akbar and Butt, 2015; Ahmed *et al.*, 2017).

It is well known that the red blood cells contain iron and they are magnetic in nature. Magnetic field can be used for a healing treatment of the patients who have stone pieces in their urinary tract (Li *et al.*, 1994). Again, the principle of magnetic field is helpful in the treatment of hypertension and certain cardiovascular disorders. On the other, Brunn (1975) suggested that the red blood cells slip at the vessel wall. In several applications, the flow pattern corresponds to a slip flow and the fluid presents a loss of adhesion at the wetted wall making the fluid slide along the wall (Kothandapani and Srinivas, 2008). Fluid shows slip effects when mean free path length of the fluid is comparable to the distance between the plates as in nanochannels or microchannels. In literature, nobody was focused on slip parameter with applied magnetic field. Keeping such fact in mind the main, objective of the study is to investigate the peristaltic flow of non-

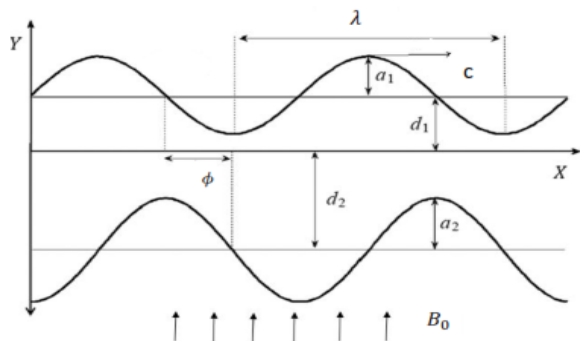


Fig. 1: Geometry of the problem

Newtonian fluid through a porous asymmetric channel with slip parameter in presence of magnetic field. The governing equations are reduced under low Reynolds number and long wave length approximation. The transformed equations have been solved numerically. Analytic solutions are also evaluated for stream function, velocity profile and pressure gradient. The effects of various important parameters are displayed graphically and discussed. The trapping phenomenon has been accorded enough attention. This result is found to be substantial importance in developing the models for blood oxygenator and hemodialysis processes.

### MATHEMATICAL FORMULATION

We consider the peristaltic motion of non-Newtonian fluid through a porous medium in two-dimensional asymmetric channel of width  $d_1 + d_2$ . Here we choose a stationary frame of reference  $(X, Y)$  such that  $X$  is selected along the axis of the channel and  $Y$  perpendicular to it. Let  $U, V$  be the velocity components in the frame  $(X, Y)$ . A sinusoidal wave with a constant speed  $c$  propagates along the channel walls. The upper and lower walls of the channel (Fig. 1) are represented by:

$$Y = H_1 = d_1 + a_1 \cos \left\{ \frac{2\pi}{\lambda} (X - ct) \right\} \quad (1)$$

$$Y = H_2 = -d_2 - a_2 \cos \left\{ \frac{2\pi}{\lambda} (X - ct) + \phi \right\} \quad (2)$$

where,  $a_1, a_2$  be the waves amplitudes,  $\lambda$  is the wave length,  $t$  is the time and  $\phi$  is the phase difference of two waves whose range is  $0 \leq \phi \leq \pi$ . It is mention that the asymmetric channel can be deduced into symmetric when  $a = b, d = 1$  and  $\phi = 0$ . Again, a uniform magnetic field strength  $B_0$  is applied in the transverse direction of the flow and then the induced magnetic field is assumed to be negligible.

The constitutive equation for Casson fluid (Eldabe *et al.*, 2001) is defined as:

$$\tau_{ij} = 2 \left( \mu_b + \frac{P_y}{\sqrt{2\pi}} \right) e_{ij} \quad (3)$$

where,  $e_{ij} = \frac{1}{2} \left( \frac{\partial v_i}{\partial x_j} + \frac{\partial v_j}{\partial x_i} \right)$  is the  $(i, j)$ th component of deformation rate,  $\tau_{ij}$  is the  $(i, j)$ th component of the stress tensor,  $\pi$  is the product of the component of deformation rate with itself and  $\mu_b$  is the plastic dynamic viscosity. The yield stress  $P_y$  is expressed as  $P_y = \frac{\mu_b \sqrt{2\pi}}{\beta}$ , where  $\beta$  Casson fluid parameter. For non-Newtonian Casson fluid flow  $\mu = \mu_b + \frac{P_y}{\sqrt{2\pi}}$  which gives  $v' = v \left( 1 + \frac{1}{\beta} \right)$ , where  $v = \frac{\mu_b}{\rho}$  is the kinematic viscosity for Casson fluid. Again, for Newtonian case  $P_y = 0$ .

With all the above-mentioned considerations, the governing equations for of non-Newtonian Casson fluid are:

$$\frac{\partial U}{\partial X} + \frac{\partial V}{\partial Y} = 0 \quad (4)$$

$$\frac{\partial U}{\partial t} + U \frac{\partial U}{\partial X} + V \frac{\partial U}{\partial Y} = -\frac{1}{\rho} \frac{\partial P}{\partial X} + v \left( 1 + \frac{1}{\beta} \right) \left( \frac{\partial^2 U}{\partial X^2} + \frac{\partial^2 U}{\partial Y^2} \right) - \frac{\sigma B_0^2}{\rho} U - v \left( 1 + \frac{1}{\beta} \right) \frac{U}{K'} \quad (5)$$

$$\frac{\partial V}{\partial t} + U \frac{\partial V}{\partial X} + V \frac{\partial V}{\partial Y} = -\frac{1}{\rho} \frac{\partial P}{\partial Y} + v \left( 1 + \frac{1}{\beta} \right) \left( \frac{\partial^2 V}{\partial X^2} + \frac{\partial^2 V}{\partial Y^2} \right) - v \left( 1 + \frac{1}{\beta} \right) \frac{V}{K'} \quad (6)$$

The corresponding boundary conditions are:

$$\left. \begin{aligned} U &= -h \frac{\partial U}{\partial Y}, & \text{at } Y = H_1 \\ U &= h \frac{\partial U}{\partial Y}, & \text{at } Y = H_2 \end{aligned} \right\} \quad (7)$$

where,

- $B_0$  = The uniform magnetic field strength
- $\sigma$  = The electric conductivity
- $\rho$  = The fluid density
- $K'$  = The permeability of the porous space
- $h$  = The velocity slip parameter

In the laboratory frame  $(X, Y)$  the flow is unsteady. But if observed in a co-ordinate system moving at the wave speed  $c$  in the wave frame  $(x, y)$ , it can be considered as steady. The co-ordinates, velocity and pressure in two frames are related to:

$$x = X - ct, y = Y, u = U - c, v = V, p = P \quad (8)$$

To minimize the complexity of the governing equations, the following non-dimension variables are used:

$$\left. \begin{aligned} x' &= \frac{x}{\lambda}, y' = \frac{y}{d_1}, u' = \frac{u}{c}, v' = \frac{v}{c\delta}, \delta = \frac{d_1}{\lambda}, t' = \frac{ct}{\lambda}, p' = \frac{pd_1^2}{\lambda c \mu_b} \\ h_1 &= \frac{H_1}{d_1}, h_2 = \frac{H_2}{d_1}, d = \frac{d_2}{d_1}, a = \frac{a_1}{d_1}, b = \frac{a_2}{d_1} \end{aligned} \right\} \quad (9)$$

The governing Eq. (4) - (6) under the assumptions of long wave length and low Reynolds number in terms of stream function  $\psi$  (dropping the das symbols) become:

$$\frac{\partial p}{\partial x} = \left(1 + \frac{1}{\beta}\right) \left[\frac{\partial^3 \psi}{\partial y^3} - \alpha^2 \left(\frac{\partial \psi}{\partial y} + 1\right)\right] \quad (10)$$

$$\frac{\partial^4 \psi}{\partial y^4} - \alpha^2 \frac{\partial^2 \psi}{\partial y^2} = 0 \quad (11)$$

$$\frac{\partial p}{\partial y} = 0 \quad (12)$$

The reduced boundary conditions are:

$$\left. \begin{aligned} \psi &= \frac{q}{2}, \quad \frac{\partial \psi}{\partial y} + \gamma \frac{\partial^2 \psi}{\partial y^2} = -1, \quad \text{at } y = h_1 = 1 + a \cos 2\pi x \\ \psi &= \frac{-q}{2}, \quad \frac{\partial \psi}{\partial y} - \gamma \frac{\partial^2 \psi}{\partial y^2} = -1, \quad \text{at } y = h_2 = -d - b \cos(2\pi x + \phi) \end{aligned} \right\} \quad (13)$$

where,

$$\alpha^2 = \frac{M^2}{1+1/\beta} + \frac{1}{K}$$

$$M = \sqrt{\frac{\sigma}{\mu_b}} B_0 d_1 = \text{The magnetic field parameter}$$

$$K = \frac{K'}{d_1^2} = \text{The permeability parameter}$$

$$q = \text{The volume flow rate in the wave frame}$$

$$Re = \frac{v}{cd_1} = \text{The Reynolds numbers}$$

$$\gamma = \frac{h}{d_1} = \text{The dimensionless velocity slip parameter}$$

### ANALYTIC SOLUTION

Equation (12) shows that pressure is a function of  $x$  only. The fourth order differential Eq. (11) subject to the boundary conditions (13) is solved for  $\psi$  and is given by:

$$\psi = C_1 + C_2 y + C_3 \cosh(\alpha y) + C_4 \sinh(\alpha y) \quad (14)$$

Also from equation (14), we get:

$$u = C_2 + C_3 \alpha \sinh(\alpha y) + C_4 \alpha \cosh(\alpha y) \quad (15)$$

where,

$$C_1 = \frac{(h_1 + h_2) \left[ q \alpha \cosh \frac{\alpha}{2} (h_1 - h_2) + (2 + q \alpha^2 \gamma) \sinh \frac{\alpha}{2} (h_1 - h_2) \right]}{-2(h_1 - h_2) \alpha \cosh \frac{\alpha}{2} (h_1 - h_2) + 2(2 - h_1 \alpha^2 \gamma + h_2 \alpha^2 \gamma) \sinh \frac{\alpha}{2} (h_1 - h_2)}$$

$$C_2 = \frac{q \alpha \cosh \frac{\alpha}{2} (h_1 - h_2) + (2 + q \alpha^2 \gamma) \sinh \frac{\alpha}{2} (h_1 - h_2)}{(h_1 - h_2) \alpha \cosh \frac{\alpha}{2} (h_1 - h_2) + (-2 + h_1 \alpha^2 \gamma - h_2 \alpha^2 \gamma) \sinh \frac{\alpha}{2} (h_1 - h_2)}$$

$$C_3 = \frac{(h_1 - h_2 + q)\sinh\frac{\alpha}{2}(h_1 + h_2)}{(h_1 - h_2)\alpha\cosh\frac{\alpha}{2}(h_1 - h_2) + (-2 + h_1\alpha^2\gamma - h_2\alpha^2\gamma)\sinh\frac{\alpha}{2}(h_1 - h_2)}$$

$$C_4 = \frac{-(h_1 - h_2 + q)\cosh\frac{\alpha}{2}(h_1 + h_2)}{(h_1 - h_2)\alpha\cosh\frac{\alpha}{2}(h_1 - h_2) + (-2 + h_1\alpha^2\gamma - h_2\alpha^2\gamma)\sinh\frac{\alpha}{2}(h_1 - h_2)}$$

Using Eq. (14), the pressure gradient is obtained from Eq. (10) and we get:

$$\frac{dp}{dx} = -(1 + 1/\beta)\alpha^2(C_2 + 1) \tag{16}$$

The volume flow rate  $q$  through each section is a constant and is given by:

$$q = \int_{h_2}^{h_1} u dy \tag{17}$$

The instantaneous flux at any axial situation is given by:

$$Q = \int_{h_2}^{h_1} (u + c) dy = q + c(h_1 - h_2) \tag{18}$$

The average flux  $\bar{Q}$  over one period ( $T = \lambda/c$ ) is defined by:

$$\bar{Q} = \frac{1}{T} \int_0^T Q dt = q + 1 + d \tag{19}$$

### NUMERICAL SOLUTION

The present problem is also solved numerically by using MATLAB software. We see that the numerical solutions agree with the analytic solutions for all the values of parameters. Figure 2 gives the comparison between the results obtained in the present study and the results of previous study (Kothandapani and Srinivas, 2008). To do so, both the studies have been brought to the same platform by considering equal parameter values (Newtonian case).

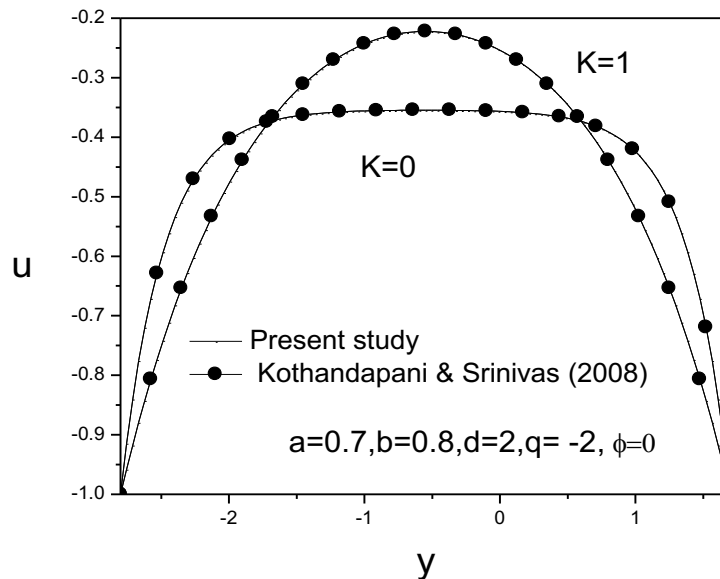


Fig. 2: Comparison of velocity profiles

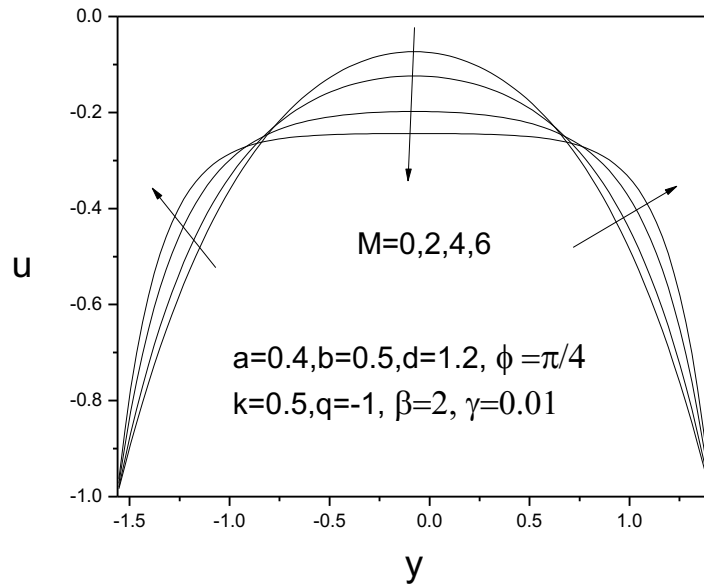


Fig. 3: Velocity profiles for different values of Magnetic field parameter  $M$

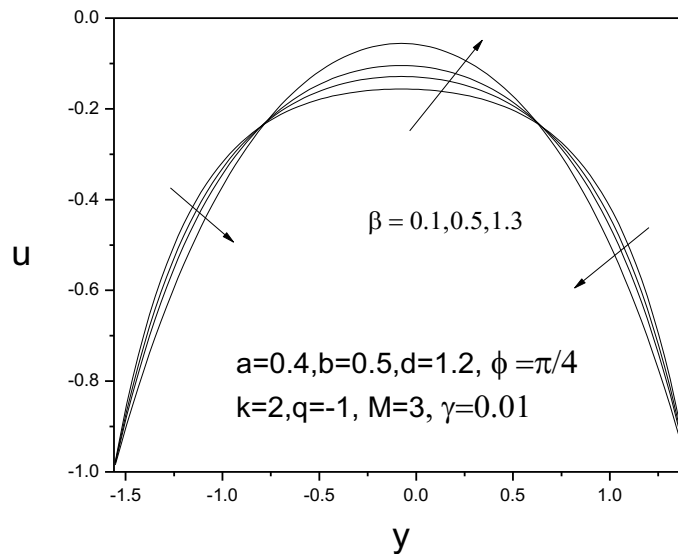


Fig. 4: Velocity profiles for different values of Casson fluid parameter  $\beta$

### RESULTS AND DISCUSSION

In this section the effect of various parameters on velocity and pressure gradient profiles are investigated. In this present study the following values are taken fixed for computations:  $a = 0.4$ ,  $b = 0.5$ ,  $d = 1.2$ ,  $q = -1$ ,  $x = 0.1$ ,  $M = 0.5$ ,  $K = 0.5$ ,  $\beta = 2$ ,  $\phi = \pi/3$  and  $\gamma = 0.01$ . All the graphs therefore correspond to these values unless specifically indicated on the appropriate figure.

Figure 3 to 6 present the velocity profiles under the effect of Magnetic field parameter ( $M$ ), Casson fluid parameter ( $\beta$ ), permeability parameter ( $K$ ) and velocity slip parameter ( $\gamma$ ). Here we see that when  $M$  is

increased, the axial velocity  $u$  increases near the walls but opposite behavior is observed in the central region of the channel. The fact is that the applied magnetic field produces a resistive force to the flow and this force reduces the velocity of the fluid. So we can say that fluid flow will be impeded if we increase the magnetic field strength. Again an increase in velocity is noticed with increase in  $\beta$  in the centre of the channel while opposite behavior is observed towards the walls as seen in Fig. 4. The Casson fluid parameter is proportional to the viscosity of fluid and thus when we increase  $\beta$  the fluid become less viscous. As a result the velocity increased at the central area. The effect of

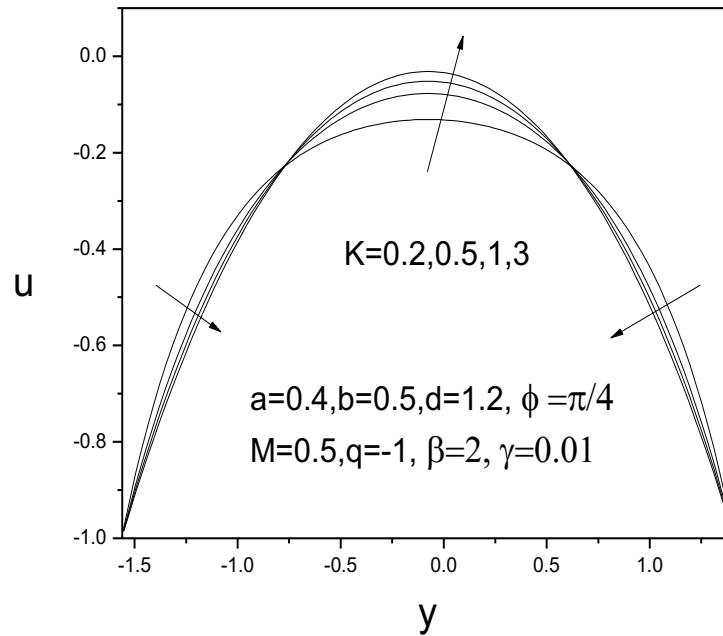


Fig. 5: Velocity profiles for different values of permeability parameter  $K$

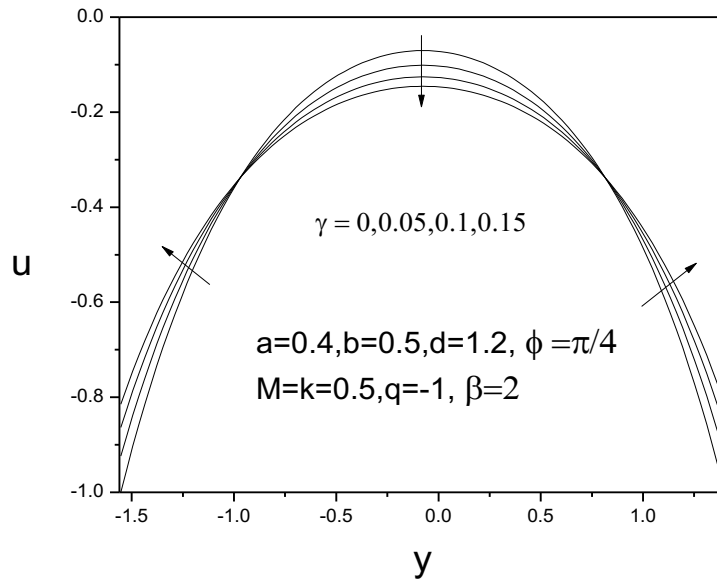


Fig. 6: Velocity profiles for different values of velocity slip parameter  $\gamma$

$K$  on velocity is displayed in Fig. 5. Here velocity increased at the central region for large  $K$ . That is, increasing  $K$  reduces the drag force and hence it causes the fluid flow to increase along the center of the channel. The influence of  $\gamma$  on velocity profiles in asymmetric channel is sketched in Fig. 6. Here we see that velocity decreases near the middle of the channel when  $\gamma$  increases but velocity increases near the wall. The reason is that the more the fluid slips at the boundary walls the less its velocity affected by the motion of the boundary.

The effects of  $M, \beta, K$  and  $\gamma$  on pressure gradient over one wave length  $x \in [0,1]$  are displayed in Fig. 7 to 10. It is observed from Fig. 7 that increasing in  $M$  increases the pressure gradient. That's meant when strong  $M$  is applied then higher-pressure gradient is needed to pass the flow of the channel. It is noted from Fig. 8 to 10 that pressure gradient decreases with an increase in  $\beta, K$  and  $\gamma$ . We know that the porosity of the channel reduces when  $K$  increases. So the pressure needed more when porosity of the channel is enhanced. On the other hand, large values of  $\gamma$  give the flow

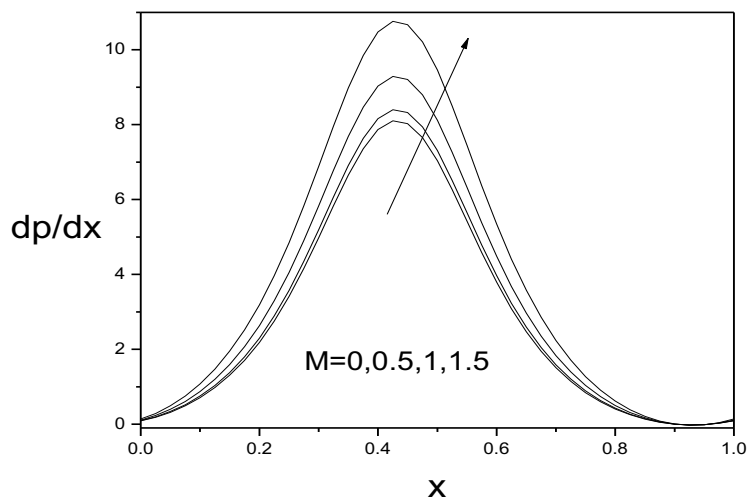


Fig. 7: Pressure gradient for different values of Magnetic field parameter  $M$

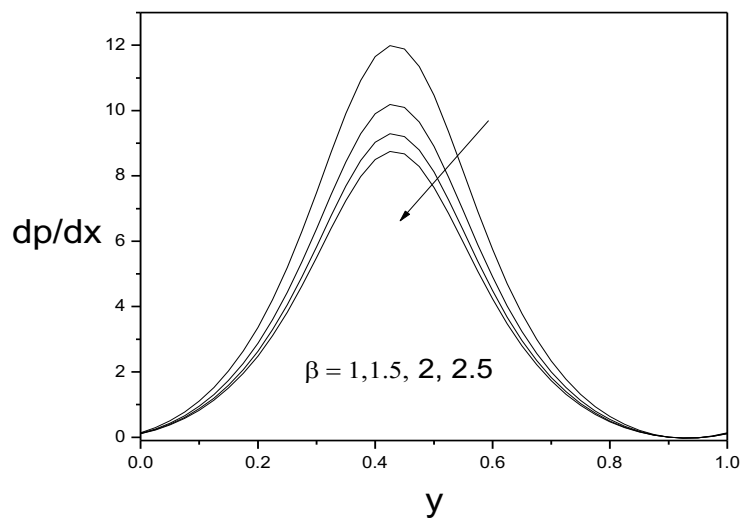


Fig. 8: Pressure gradient for different values of Casson fluid parameter  $\beta$

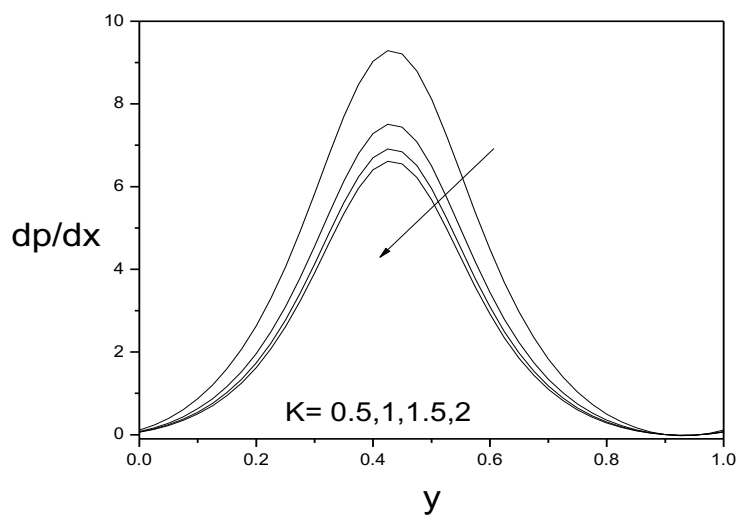


Fig. 9: Pressure gradient for different values of permeability parameter  $K$

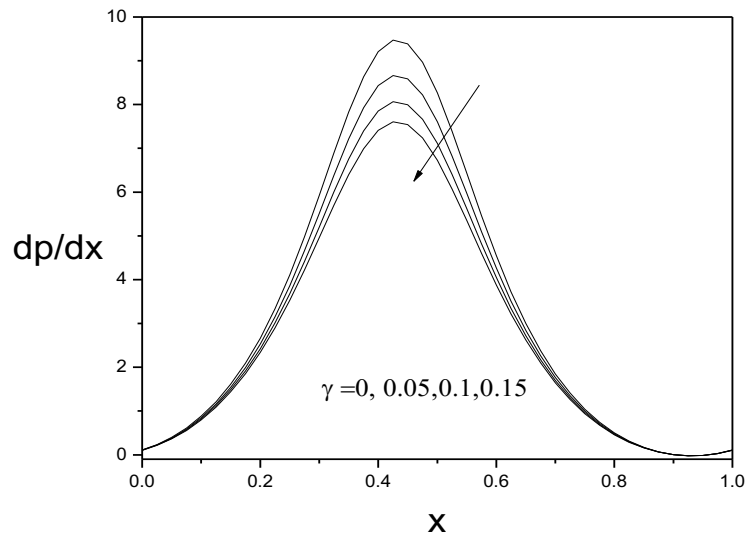


Fig. 10: Pressure gradient for different values of velocity slip parameter  $\gamma$

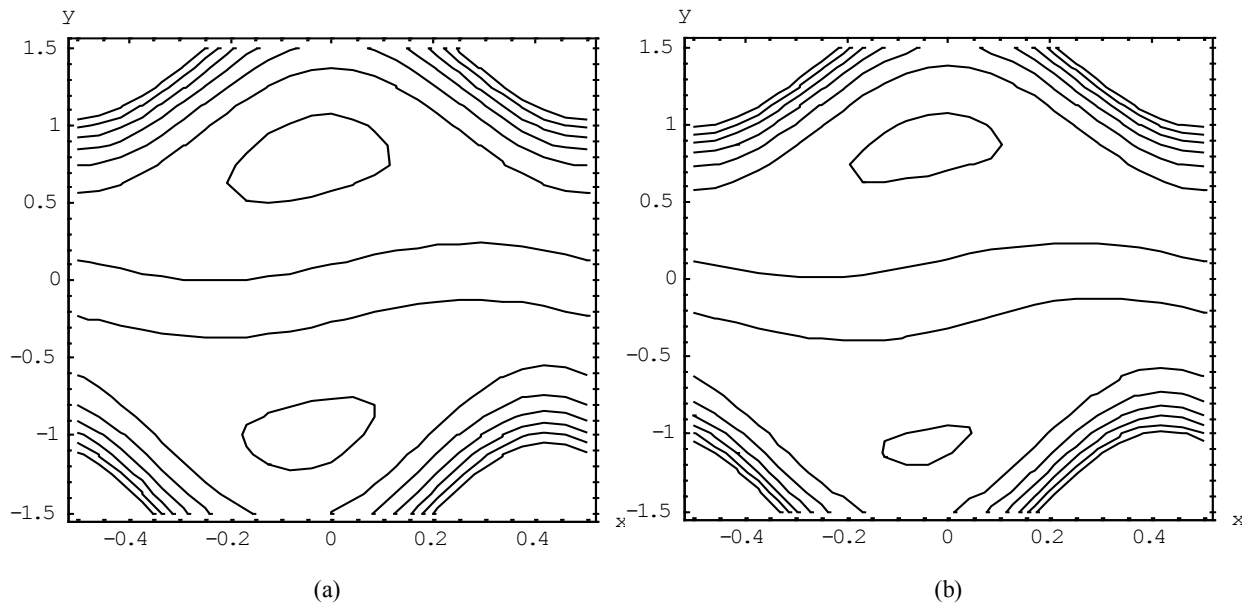


Fig. 11: Stream lines for  $M, a = 0.4, b = 0.5, d = 1.1, K = 1, \beta = 2, \gamma = 0.1, \bar{Q} = 2.2, \phi = 0.5, (a) M = 0, (b) M = 2$

transport towards Newtonian. Consequently, pressure gradient decreased with large  $\gamma$ .

Another interesting phenomenon for peristaltic flow is trapping. It is the structure of an internally circulating bolus of fluid by closed streamlines. The effect of Magnetic field parameter  $M$  on trapping is explained in Fig. 11. It is noted that the size of the trapped bolus decreases with increase of  $M$ . This is due to the fact that when we increased  $M$  then the electromagnetic forces are higher than the viscous forces and this electromagnetic force causes the resistance in the flow of the fluid. The influence of velocity slip parameter  $\gamma$  on streamlines is seen in Fig. 12. Here we see that two circulating trapped boluses exist near the wall and the size of the bolus decreases with an increase in  $\gamma$ . Figure 13 is sketched to see the

property of streamlines for different values of Casson fluid parameter  $\beta$ . The fluid becomes less viscous and becomes less thick when we increase the value of  $\beta$ . So, it can be concluded that the volume of the trapping bolus increases with increasing  $\beta$ . Figure 14 describes the effect of phase difference  $\phi$  on streamlines for symmetric ( $a = b, d = 1, \phi = 0$ ) and asymmetric channel. This figure shows that the trapped bolus appearing in the middle of the channel for  $\phi = 0$  moves towards left and decreases in size as  $\phi$  increase.

## CONCLUSION

In this study, we have discussed peristaltic flow of non-Newtonian fluid through a porous asymmetric

channel under the influence of magnetic field. Velocity slip effect was considered. Both analytic and numerical solutions for stream function, velocity and pressure gradient have been developed. The features of flow characteristics are analyzed and discussed by sketching graphs. We have concluded the following important conclusions:

- Velocity field decreases at the central region of the channel and increases near the wall for increasing  $\gamma$  and  $M$ .

- Magnitude of pressure gradient increases with increasing  $M$  while decreases with  $\beta$  and  $K$ .
- The size of the trapped bolus decreases with increasing  $\gamma$ .

### ACKNOWLEDGMENT

The authors are thankful to the reviewers for their kind words and constructive suggestions. The corresponding author is thankful to UGC, Dhaka, Bangladesh for awarding him a research fellowship.

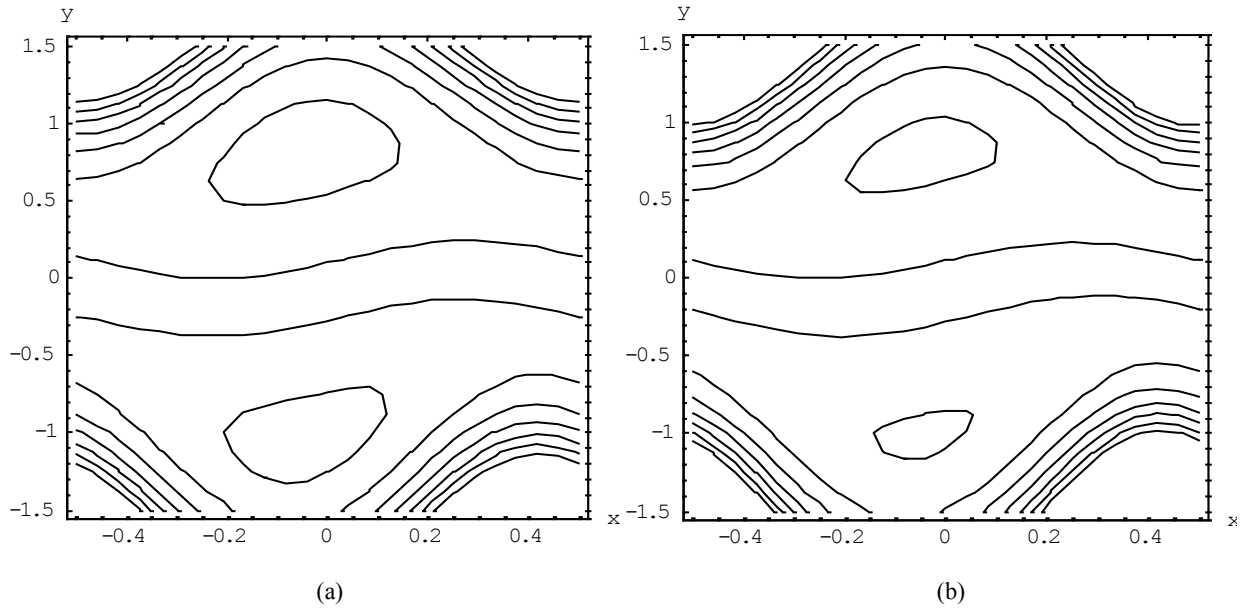


Fig. 12: Stream lines for  $\gamma$ ,  $a = 0.4, b = 0.5, d = 1.1, K = M = 1, \beta = 2, \bar{Q} = 2.2, \phi = 0.5$ , (a)  $\gamma = 0$ , (b)  $\gamma = 0.2$

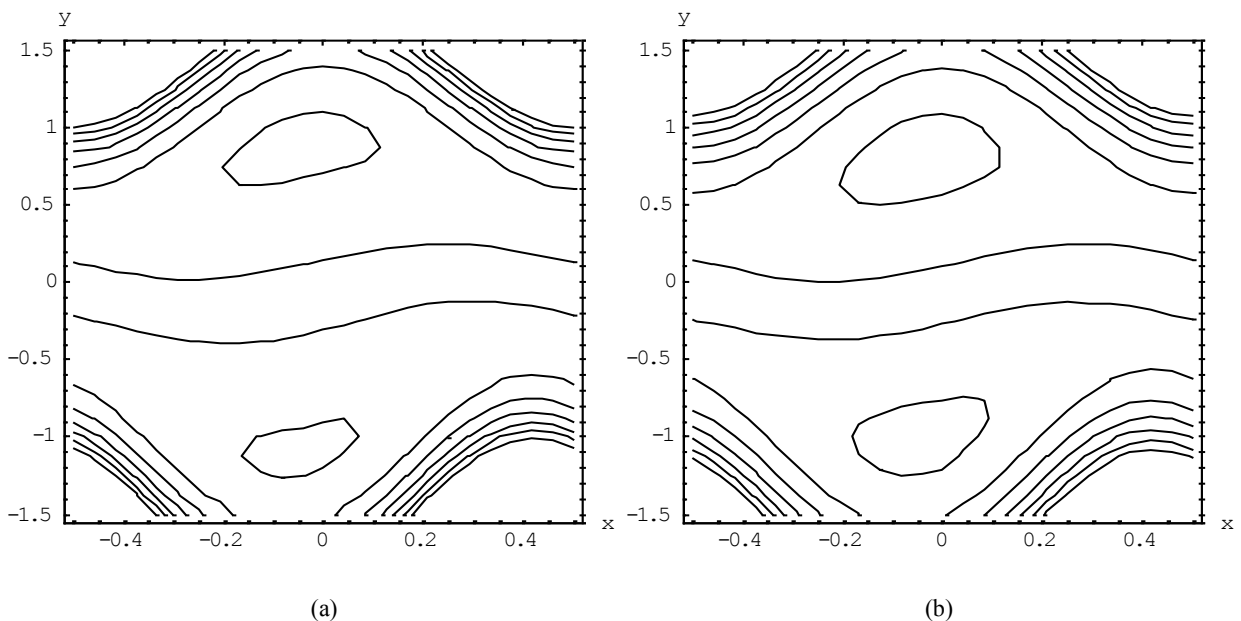


Fig. 13: Stream lines for  $\beta$ ,  $a = 0.4, b = 0.5, d = 1.1, K = 1, M = 2.5, \bar{Q} = 2.2, \phi = 0.5, \gamma = 0.1$ , (a)  $\beta = 0.5$ , (b)  $\beta = 2$

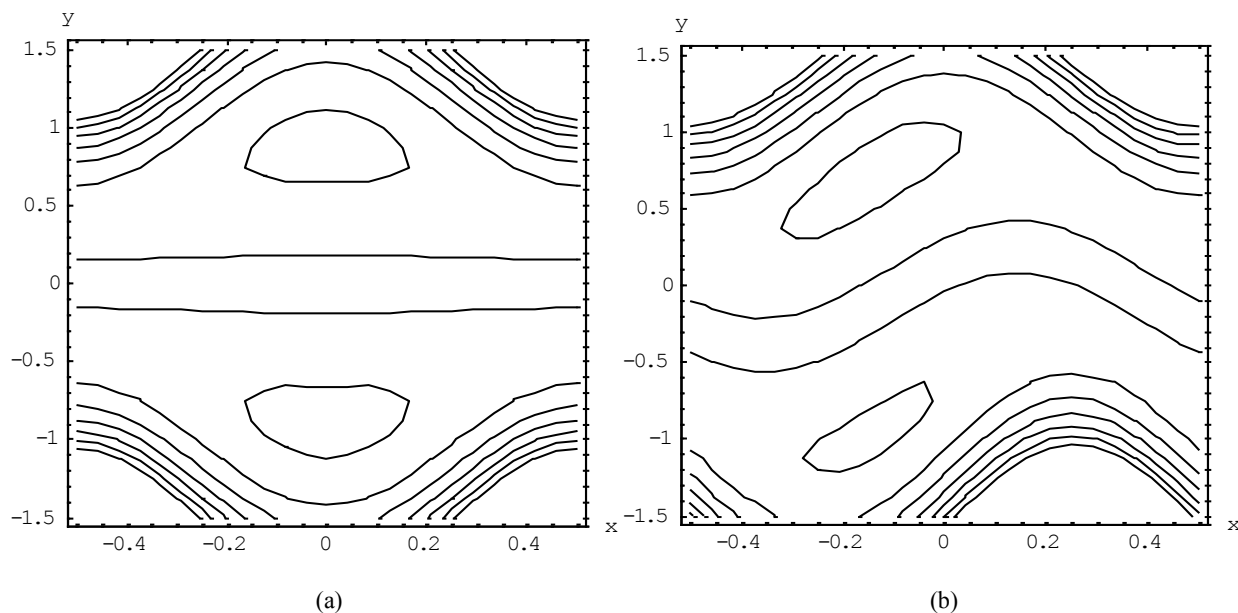


Fig. 14: Stream lines for  $\phi$ ,  $M = K = 1, \bar{Q} = 2.2, \beta = 2, \gamma = 0.1$  (a)  $a = b = 0.4, d = 1, \phi = 0$ , (b)  $a = 0.4, b = 0.5, d = 1.1, \phi = \pi/2$

### REFERENCES

- Abd-Alla, A.M., S.M. Abo-Dahab and R.D. Al-Simery, 2013. Effect of rotation on peristaltic flow of a micropolar fluid through a porous medium with an external magnetic field. *J. Magn. Mater.*, 348: 33-43.
- Ahmed, B., T. Javed, A.H. Hamid and M. Sajid, 2017. Numerical analysis of mixed convective peristaltic flow in a vertical channel in presence of heat generation without using lubrication theory. *J. Appl. Fluid Mech.*, 10(6): 1813-1827.
- Akbar, N.S. and A.W. Butt, 2015. Physiological transportation of Casson fluid in a plumb duct. *Commun. Theor. Phys.*, 63(3): 347-352.
- Brunn, P., 1975. The velocity slip of polar fluids. *Rheol. Acta*, 14(12): 1039-1054.
- Casson, N., 1959. *Rheology of Disperse Systems*. Pergamon Press, London, pp: 84.
- De Vries, K., E.A. Lyons, G. Ballard, C.S. Levi and D.J. Lindsay, 1990. Contractions of the inner third of the myometrium. *Am. J. Obstet. Gynecol.*, 162(3): 679-682.
- Elangovan, K. and K. Selvaraj, 2017. MHD peristaltic flow of blood through porous medium with slip effect in the presence of body acceleration. *World J. Modell. Simulat.*, 13(02): 151-160.
- Eldabe, N.T.M., G. Saddeek and A.F. El-Sayed, 2001. Heat transfer of MHD non-Newtonian Casson fluid flow between two rotating cylinders. *Mech. Mechan. Eng.*, 5(2): 237-251.
- Kothandapani, M. and S. Srinivas, 2008. Non-Linear peristaltic transport of a Newtonian fluid in an inclined asymmetric channel through a porous medium. *Phys. Lett. A*, 372: 1265-1276.
- Latham, T.W., 1966. Fluid motion in a peristaltic pump. M.S. Thesis, MIT, Cambridge, MA.
- Li, A.A., N.I. Nesterov, S.N. Malikova and V.A. Kiiatkin, 1994. The use of an impulse magnetic field in the combined therapy of patients with stone fragments in the upper urinary tract. *Vopr. Kurortol. Fizioter. Lech. Fiz. Kult.*, 3: 22-24.
- Mishra, M. and A.R. Rao, 2003. Peristaltic transport of a Newtonian fluid in an asymmetric channel. *Z. Angew. Math. Phys.*, 54: 532-550.
- Nadeem, S., Rizwan Ul Haq and C. Lee, 2012. MHD flow of a Casson fluid over an exponentially shrinking sheet. *Sci. Iran.*, 19(6): 1550-1553.
- Nagarani, P., 2010. Peristaltic transport of a Casson fluid in an inclined channel. *Korea-Australia Rheol. J.*, 22(2): 105-111.
- Pandey, S.K. and D. Tripathi, 2011. A mathematical model for swallowing of concentrated fluids in oesophagus. *Appl. Bionics Biomech.*, 8: 309-321.
- Srinivas, S. and V. Pushparaj, 2008. Non-linear peristaltic transport in an inclined asymmetric channel. *Commun. Nonlinear Sci.*, 13(9): 1782-1795.
- Tripathi, D., 2011. A mathematical model for the peristaltic flow of chyme movement in small intestine. *Math. Biosci.*, 233(2): 90-97.